NIH Public Access
Author Manuscript
J Am Chem Soc. Author manuscript; available in PMC 2013 December 21.

Published in final edited form as:
J Am Chem Soc. 2007 June 20; 129(24): . doi:10.1021/ja072528a.

The active form of *Chlamydia trachomatis* ribonucleotide reductase R2 protein contains a heterodinuclear Mn(IV)/Fe(III) cluster with *S* = 1 ground state

Wei Jiang, **J. Martin Bollinger Jr.**[*], and **Carsten Krebs**[*]
Department of Biochemistry and Molecular Biology and Department of Chemistry, The Pennsylvania State University, University Park, Pennsylvania 16802

Abstract

The class I ribonucleotide reductase from *Chlamydia trachomatis* uses a stable Mn^{IV}/Fe^{III} cofactor to initiate nucleotide reduction by a free-radical mechanism. The enzyme provides the first example both of a Mn-dependent ribonucleotide reductase and of a Mn/Fe redox cofactor. In this work, we have used variable-field Mössbauer spectroscopy to demonstrate that the active cofactor has an $S = 1$ ground state due to antiferromagnetic coupling between the Mn^{IV} ($S_{Mn} = 3/2$) and high-spin Fe^{III} ($S_{Fe} = 5/2$) sites.

The reduction of nucleotides to 2′-deoxynucleotides by ribonucleotide reductases (RNRs)[1] begins with the abstraction of the 3′ hydrogen atom of the substrate by a transient cysteine thiyl radical (C•).[2–4] Class I, II, and III RNRs differ in subunit composition and the nature of the cofactor used to generate the 3′-H-abstracting C•.[2] A conventional class I RNR uses a stable tyrosyl radical (Y•), which is introduced into the enzyme's homodimeric R2 subunit (also denoted β_2) by reaction of O_2 with an adjacent carboxylate-bridged non-heme diiron cluster,[5] to generate the C• in its R1 subunit (also denoted α_2) via long-range (~ 35 Å) proton-coupled electron transfer (PCET).[6–8] The identification in *Chlamydia trachomatis* (*Ct*) and other species of pathogenic bacteria of RNRs having the class I subunit architecture but the Y•-harboring tyrosine replaced by phenylalanine raised the question of how such an RNR might function without the initiating Y•.[9,10] We recently showed that *Ct* RNR uses a stable Mn^{IV}/Fe^{III} cofactor, generated by reaction of the Mn^{II}/Fe^{II}-R2 complex with O_2, for radical initiation.[11] Although heterobinuclear Mn/Fe complexes of various oxidation states,[12–14] including one example of an inorganic Mn^{IV}/Fe^{III} complex,[15] have been reported, *Ct* RNR is, to our knowledge, the first case in which an enzyme has been shown to use a Mn/Fe cluster as a redox cofactor. Here we characterize this novel cofactor by Mössbauer spectroscopy, showing that it has a triplet ($S_{Total} = 1$) ground state resulting from antiferromagnetic coupling of its Mn^{IV} ($S_{Mn} = 3/2$) and high-spin Fe^{III} ($S_{Fe} = 5/2$) constituents and providing parameters to calibrate calculation of its geometric and electronic structure.

The 4.2-K/zero-field Mössbauer spectrum of a sample prepared by reaction of a solution of R2, Mn^{II}, and Fe^{II} with O_2[16] (Figure 1, hashed marks) comprises two quadrupole doublets with similar isomer shifts (δ) but different quadrupole splittings (ΔE_Q). The minor doublet

ckrebs@psu.edu or jmb21@psu.edu.

Supporting Information Available: Rationale for method of sample preparation, component analysis to resolve the spectra of Mn^{IV}/Fe^{III}-R2 shown in Figure 2, analysis of these spectra for the hypothetical case of an $S_{Total} = 4$ ground state, selected plots of the spin expectation values, and the spin Hamiltonian used for analysis of the Mössbauer spectra. This material is available free of charge from the journal website: http://pubs.acs.org.

NIH-PA Author Manuscript
NIH-PA Author Manuscript
NIH-PA Author Manuscript

NIH-PA Author Manuscript

NIH-PA Author Manuscript

NIH-PA Author Manuscript

(25% of the total intensity) matches the spectrum of the $Fe_2^{III/III}$ cluster, which is characterized by $\delta = 0.50$ mm/s and $\Delta E_Q = 0.79$ mm/s (Figure 1, solid line). The major doublet (75% intensity) arises from the functional Mn^{IV}/Fe^{III} cofactor.[11] For in-depth characterization of this species, we collected Mössbauer spectra at 4.2 K in variable applied magnetic fields. To analyze these spectra, it was necessary first to remove the 25% contribution attributed to the $Fe_2^{III/III}$ complex (Figure S1). The derived spectra of the Mn^{IV}/Fe^{III} complex are shown in Figure 2.

The zero-field spectrum is a sharp quadrupole doublet with parameters ($\delta = 0.52$ mm/s and $\Delta E_Q = 1.32$ mm/s) typical of high-spin Fe^{III}. Spectra recorded in applied fields were analyzed with the assumption of slow relaxation and according to the spin Hamiltonian with respect to the total-spin ground state, $S_{Total} = 1$, given in the Supporting Information. For this analysis, the parameters determined from the zero-field spectrum were fixed. The other parameters in the simulations are the asymmetry parameter, η, the axial and rhombic zero-field splitting (ZFS) parameters of the $S_{Total} = 1$ ground state, $D_{S=1}$ and $(E/D)_{S=1}$, respectively, and the hyperfine tensor for the Fe^{III} ion, $(\mathbf{A}/g_N\beta_N)_{Fe}$.

The fact that the overall splitting of the spectrum is larger at 4 T than at 8 T reveals that the electronic Zeeman term dominates the ZFS interaction at these magnetic field strengths. As a consequence, the spin expectation value of the ground state ($\langle S \rangle$) and the internal magnetic field [$B_{int} = -\langle S \rangle \cdot (\mathbf{A}/g_N\beta_N)_{Fe}$] approach their limiting values (corresponding to $\langle S \rangle = -1$) at these applied fields, and the hyperfine tensor can be determined accurately from the spectra. In a spin-coupled cluster, the **A**-tensor for the iron ion with respect to the $S_{Total} = 1$ ground state ($\mathbf{A}_{Fe}$) is given by equation 1, in which c_{Fe} and $\mathbf{a}_{Fe}$ represent the vector coupling coefficient and the intrinsic hyperfine tensor, respectively.[17]

$$\mathbf{A}_{Fe} = c_{Fe}\,\mathbf{a}_{Fe} \quad (1)$$

For high-spin Fe^{III} sites, $(\mathbf{a}/g_N\beta_N)_{Fe}$ is dominated by the Fermi contact term and exhibits nearly isotropic values of ~ −21 T.[18] For the $S_{Total} = 1$ state, $c_{Fe} = +7/4$. Thus, $(\mathbf{A}/g_N\beta_N)_{Fe}$ is expected to be nearly isotropic with values of ~ −37 T. Indeed, analysis of the spectra yielded a nearly isotropic hyperfine tensor, $(\mathbf{A}/g_N\beta_N)_{Fe} = (-40.2, -38.9, -38.0)$ T, similar to the expected value.

With the $\mathbf{A}_{Fe}$ determined from the 4-T and 8-T spectra, the ZFS-parameters were then determined accurately from the spectra with lesser applied magnetic fields, under which conditions the ZFS is significant compared to the electronic Zeeman term. Simulation of the spectra provided for determination of the magnetic-field dependence of $\langle S \rangle$, which determines the magnitude of the internal magnetic field and the resultant splitting in each spectrum. From the field-dependent spectra, $D_{S=1} = -1.9$ cm^{-1} and $(E/D)_{S=1} = 0.33$ were found. $D_{S=1}$ is related to the intrinsic D-values of the Mn^{IV} and Fe^{III} ions via equation 2, with the assumption that the total spin states are well separated in energy (i.e., $J \gg D$).[17]

$$D_{S=1} = 14/5\, D_{Fe} + 3/10\, D_{Mn} \quad (2)$$

$D_{S=1}$ is dominated by the contribution from the Fe^{III} site[19] and can be rationalized with a value typical for high-spin Fe^{III} ($|D_{Fe}|$ of ~ 0.7 cm^{-1}).[18]

The Mn^{IV} and Fe^{III} ions could conceivably couple ferromagnetically to yield an $S_{Total} = 4$ ground state. However, the inherent anisotropy of $\langle S \rangle$ of the $S_{Total} = 4$ system precludes simulation of all the experimental spectra with a single set of spin-Hamiltonian parameters. Specifically, comparison of the 4-T and 8-T spectra establishes that $\langle S \rangle$ along all three

NIH-PA Author Manuscript

NIH-PA Author Manuscript

NIH-PA Author Manuscript

molecular axes nearly reach saturation in an applied field of ~4 T. $|D_{S=4}|$ would therefore have to be small (< 0.5 cm^{-1}, see Figure S2). Conversely, with a $D_{S=4}$ of this small magnitude, $\langle S_z \rangle$ (for $D_{S=4} < 0$) saturates at ~30 mT (Figure S2), resulting in much greater magnetic hyperfine splitting in the weak-field spectra than is observed (Figure S3). Thus, ferromagnetic coupling to yield $S_{Total} = 4$ can be ruled out.

The demonstration by Mössbauer spectroscopy that the Mn^{IV}/Fe^{III} cluster in the active form of *Ct* R2 has a $S_{Total} = 1$ ground state arising from antiferromagnetic coupling between the $S_{Mn} = 3/2$ and $S_{Fe} = 5/2$ ions represents an important first step toward defining its electronic structure. Moreover, parameters obtained in the analysis can now be used to calibrate density functional theory calculations to extract deeper insight.[20,21] This insight will permit an important unresolved aspect of class I RNR function – how electron transfer to the oxidized cofactor in R2 is "gated" so as to occur only in the active holoenzyme complex – to be addressed. Direct interrogation of the radical initiation step in conventional class I RNRs has proven to be extremely challenging.[7] The R2 product of radical transfer does not accumulate during turnover because of unfavorable kinetics.[7,22] Accumulation of the reduced cofactor can be promoted by use of radical-trapping substrate analogues or R1 variants,[23–26] but extracting atomic-level insight into the changes to the cofactor upon reduction is not straightforward. The reduced Y lacks a useful spectroscopic signature. The $Fe_2^{III/III}$ cluster is either unchanged by the radical-transfer step or, at most, may transfer a proton to the Y from a coordinated water ligand, a change not obviously demonstrable by the spectroscopic methods to which the EPR-silent cluster is amenable. The use of the novel cofactor by *Ct* RNR affords a unique opportunity to dissect the initiation step. The metal cluster undergoes reduction from Mn^{IV}/Fe^{III} to Mn^{III}/Fe^{III}, which is, by contrast to the reduced cofactor of a conventional class I RNR, *EPR active*.[11] Moreover, although the reduced form might, as in *E. coli* RNR, not accumulate during turnover, it can be prepared in stable form and its structure is affected by binding of R1 and nucleotides, as demonstrated by marked changes to its EPR spectrum.[11] The structural changes caused by formation of the complex are almost certainly elements of the gating mechanism. By defining what they are and extending the description of the geometric and electronic structure of the Mn^{IV}/Fe^{III} cofactor initiated by this work, insight into the mechanisms of radical transfer and conformational gating thereof may be obtained.

Supplementary Material

Refer to Web version on PubMed Central for supplementary material.

Acknowledgments

This work was supported by the National Institutes of Health (GM-55365 to JMB), the Beckman Foundation (Young Investigator Award to CK), and the Dreyfus Foundation (Teacher Scholar Award to CK).

References

1. Abbreviations used: *Ct: Chlamydia trachomatis*; PCET: proton-coupled electron transfer; RNR: ribonucleotide reductase; ZFS: zero field splitting.
2. Licht S, Gerfen GJ, Stubbe J. Science. 1996; 271:477–481. [PubMed: 8560260]
3. Stubbe J. Curr Opin Struct Biol. 2000; 10:731–736. [PubMed: 11114511]
4. Nordlund P, Reichard P. Annu Rev Biochem. 2006; 75:681–706. [PubMed: 16756507]
5. Atkin CL, Thelander L, Reichard P. J Biol Chem. 1973; 248:7464–7472. [PubMed: 4355582]
6. Stubbe J, Riggs-Gelasco P. Trends Biochem Sci. 1998; 23:438–443. [PubMed: 9852763]
7. Stubbe J, Nocera DG, Yee CS, Chang MCY. Chem Rev. 2003; 103:2167–2202. [PubMed: 12797828]

NIH-PA Author Manuscript

NIH-PA Author Manuscript

NIH-PA Author Manuscript

8. Stubbe J. Curr Opin Chem Biol. 2003; 7:183–188. [PubMed: 12714050]
9. Roshick C, Iliffe-Lee ER, McClarty G. J Biol Chem. 2000; 275:38111–38119. [PubMed: 10984489]
10. Högbom M, Stenmark P, Voevodskaya N, McClarty G, Gräslund A, Nordlund P. Science. 2004; 305:245–248. [PubMed: 15247479]
11. Jiang W, Yun D, Saleh L, Barr EW, Xing G, Hoffart LM, Maslak M-A, Krebs C, Bollinger JM Jr. Science. 2007 accepted.
12. Bossek U, Weyhermüller T, Wieghardt K, Bonvoisin J, Girerd JJ. J Chem Soc, Chem Comm. 1989:633–636.
13. Schenk G, Boutchard CL, Carrington LE, Noble CJ, Moubaraki B, Murray KS, De Jersey J, Hanson GR, Hamilton S. J Biol Chem. 2001; 276:19084–19088. [PubMed: 11278566]
14. Pierce BS, Hendrich MP. J Am Chem Soc. 2005; 127:3613–3623. [PubMed: 15755183]
15. Hotzelmann R, Wieghardt K, Flörke U, Haupt HJ, Weatherburn DC, Bonvoisin J, Blondin G, Girerd JJ. J Am Chem Soc. 1992; 114:1681–1696.
16. An anaerobic solution of R2 (3.0 mM β), Mn^{II} (3.0 mM), and Fe^{II} (1.5 mM) in 100 mM HEPES (pH = 7.6) containing 10% (v/v) glycerol was mixed at 5 °C with an equal volume of an O_2-saturated solution of the same buffer, and the reaction was allowed to proceed for 10 min before the sample was frozen. The control sample was prepared identically, except the Mn^{II} was omitted and the concentration of Fe^{II} was doubled in the protein reactant solution. See the Supporting Information for a discussion of the logic underlying the method of sample preparation.
17. Bencini, A.; Gatteschi, D. EPR of exchange coupled systems. Springer; Berlin, Germany: 1990.
18. Münck, E. Physical Methods in Bioinorganic Chemistry. Que, L., Jr, editor. University Science Books; Sausalito, CA: 2000. p. 287-319.
19. High-spin Fe^{III} and Mn^{IV} have well-isolated, non-degenerate orbital ground states and typically exhibit small intrinsic *D*-values.
20. Han WG, Liu T, Lovell T, Noodleman L. J Inorg Biochem. 2006; 100:771–779. [PubMed: 16504298]
21. Sinnecker S, Svensen N, Barr EW, Ye S, Bollinger JM Jr, Neese F, Krebs C. J Am Chem Soc. 2007 accepted.
22. Ge J, Yu G, Ator MA, Stubbe J. Biochemistry. 2003; 42:10071–10083. [PubMed: 12939135]
23. Thelander L, Larsson B, Hobbs J, Eckstein F. J Biol Chem. 1976; 251:1398–1405. [PubMed: 767333]
24. Mao SS, Johnston MI, Bollinger JM, Stubbe J. Proc Natl Acad Sci U S A. 1989; 86:1485–1489. [PubMed: 2493643]
25. Persson AL, Eriksson M, Katterle B, Pötsch S, Sahlin M, Sjöberg BM. J Biol Chem. 1997; 272:31533–31541. [PubMed: 9395490]
26. Stubbe J, van der Donk WA. Chem Rev. 1998; 98:705–762. [PubMed: 11848913]

NIH-PA Author Manuscript

NIH-PA Author Manuscript

NIH-PA Author Manuscript

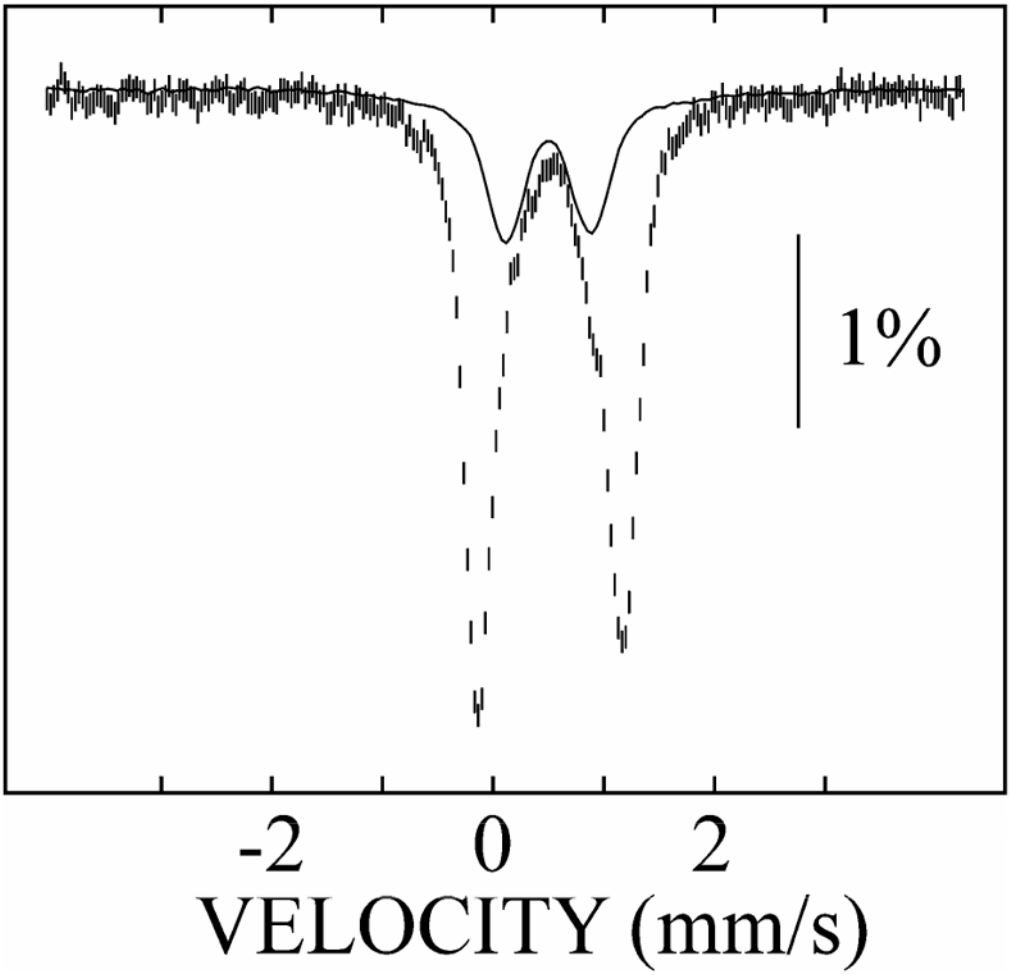

Figure 1.

4.2-K/zero-field Mössbauer spectrum of the final product of the reaction of Mn^{II}/Fe^{II} *Ct*-R2 with O_2 (hashed marks). The solid line is the spectrum of the final product of the reaction of Fe^{II}/Fe^{II} *Ct*-R2 with O_2 (25% of the total intensity).

NIH-PA Author Manuscript
NIH-PA Author Manuscript
NIH-PA Author Manuscript

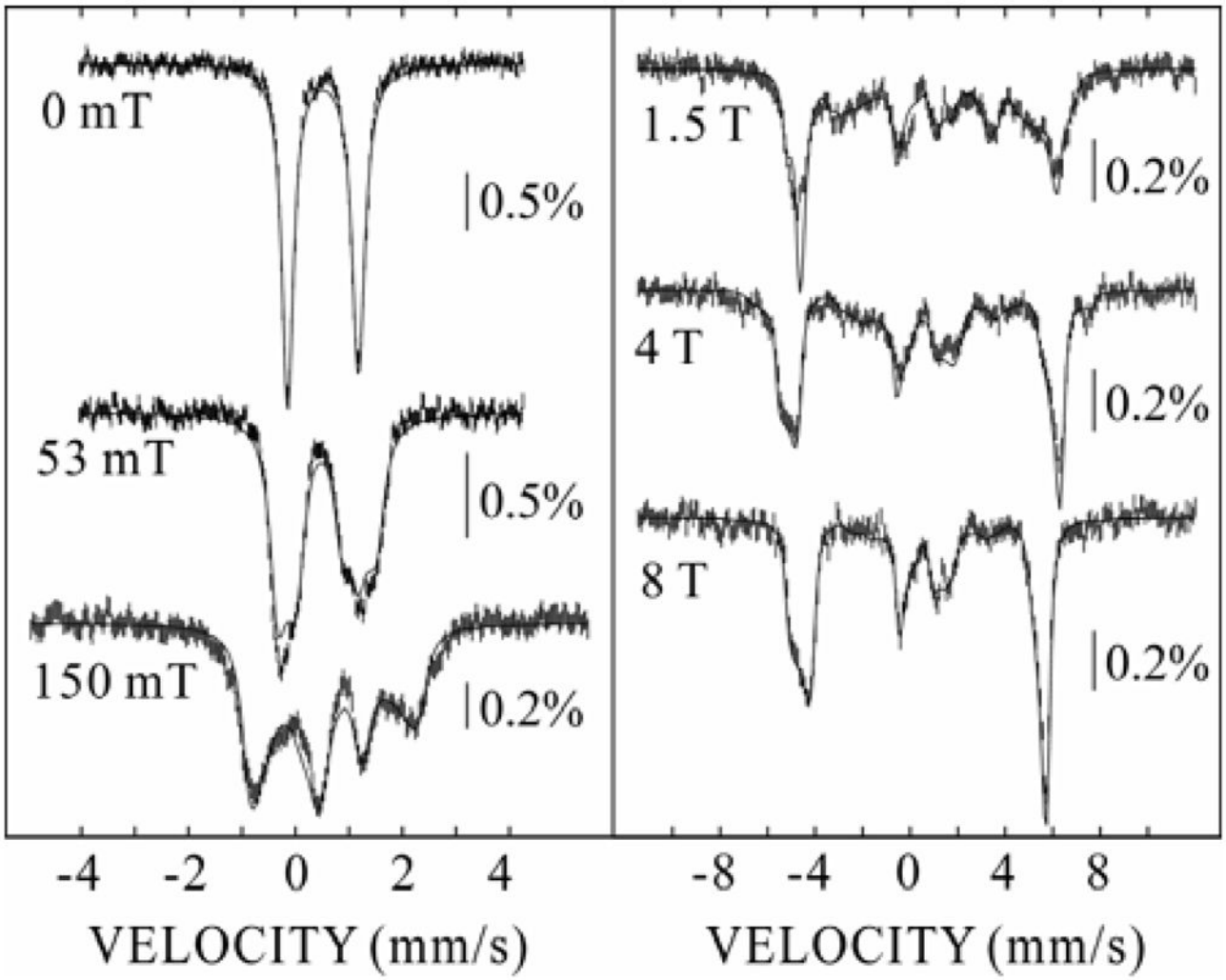

Figure 2.

4.2-K Mössbauer spectra of Mn^{IV}/Fe^{III}-R2 derived by component analysis of the experimental spectra. The solid lines are simulations according to the spin Hamiltonian given in the Supporting Information and the following parameters: $S_{Total} = 1$, $D_{S=1} = -1.9$ cm^{-1}, $(E/D)_{S=1} = 0.33$, $\delta = 0.52$ mm/s, $\Delta E_Q = 1.32$ mm/s, $\eta = -2.6$, $(\mathbf{A}/g_N\beta_N)_{Fe} = (-40.2, -38.9, -38.0)$ T.

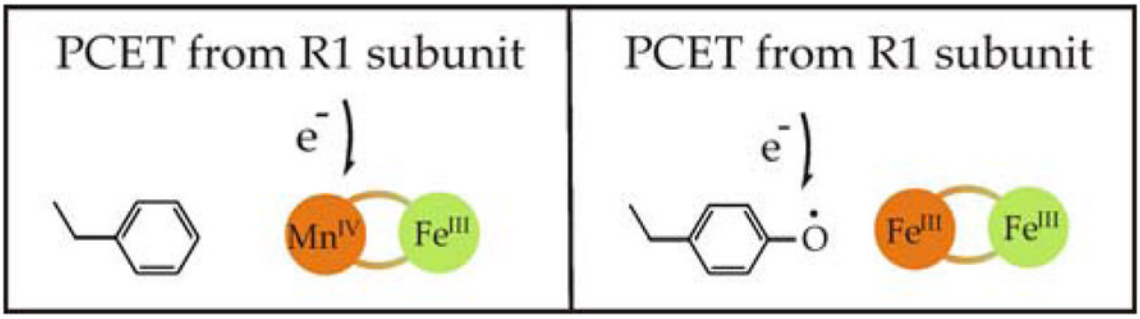

Scheme 1.
Radical-generating cofactor of *Ct* RNR (left) and conventional class I RNR (right).

NIH-PA Author Manuscript
NIH-PA Author Manuscript
NIH-PA Author Manuscript